Proceedings of the Seventh International Conference on
Railway Technology: Research, Development and Maintenance
Edited by: J. Pombo
Civil-Comp Conferences, Volume 15, Paper 10.2
Civil-Comp Press, Edinburgh, United Kingdom, 2026
ISSN: 2753-3239, doi: 10.4203/ccc.15.10.2

Indirect Measurement of the Contact Force in Laboratory Pantograph Tests

J. Gil, M. Tur, S. Gregori, A. M. Pedrosa and F. J. Fuenmayor

Mechanical Engineering and Biomechanics University Research Institute (I2MB), Universitat Politècnica de València, Valencia, Spain

Abstract

The contact force between the pantograph and the overhead contact line is a fundamental indicator of the mechanical performance of railway current collection systems. Existing measurement techniques rely on instrumented pantographs, requiring structural modifications that increase system complexity and limit large-scale deployment. This paper presents and experimentally validates a fully non-intrusive methodology for estimating the pantograph contact force using acceleration, displacement, and pressure measurements only.

The proposed strategy decomposes the estimation problem into two frequency domains. The very low-frequency component of the contact force is reconstructed from the pressure signal of the pantograph uplift mechanism, while the remaining frequency content is solved by an inverse dynamic problem based on acceleration and displacement measurements. Contact force estimation is performed using Kalman-filter-based models, and three different formulations are investigated and compared. Model parameters are optimised to ensure a fair assessment of each approach. Two sensing configurations are considered: combined acceleration and displacement measurements, and acceleration-only measurements.

The methodology is validated experimentally using a laboratory test bench equipped with a real pantograph, where the estimated contact force is compared with a reference force measured at the application point.

Keywords: pantograph–catenary interaction, inverse dynamics, indirect force estimation, augmented Kalman filter, optimisation, monitoring.

1 Introduction

1.1 Background

Electric trains collect power through a pantograph that maintains sliding contact with the overhead contact line (OCL). The mechanical quality of this interaction is commonly assessed by the time-varying contact force (CF) at the pantograph–catenary interface. For this reason, extensive research has been devoted to predictive modelling of the contact force [3], as well as to its experimental measurement for homologation and condition monitoring purposes [8].

Due to the sliding nature of the contact, direct measurement of the contact force is not feasible. Industrial practice therefore relies on instrumented pantographs, where force transducers are integrated into the structure and combined with correction procedures based on additional measurements. Although effective, this approach requires structural modifications of the pantograph, increasing cost and limiting applicability. As a result, there is increasing interest in alternative measurement strategies that avoid any modification of the pantograph structure.

1.2 Problem of interest

This work addresses the problem of estimating the contact force acting on an operating pantograph without altering its structural components. Only acceleration and displacement measurements are considered for the indirect estimation of the contact force, which requires solving an inverse dynamic problem. In this study, classical model-based approaches are adopted.

Acceleration and displacement signals alone are insufficient to recover the mean value and very low-frequency components of the contact force. To overcome this limitation, the pressure signal of the pantograph uplift mechanism is exploited to reconstruct the low-frequency content of the force. The proposed methodology is experimentally evaluated using a laboratory test bench equipped with a real pantograph, where the estimated force can be directly compared with a reference measurement.

In accordance with the European Standard EN 50317 [8], which specifies a contact force evaluation bandwidth of 0–20 Hz, the present study focuses on force estimation within this frequency range.

1.3 Literature review

Contact force measurement in pantograph–catenary systems is regulated by the European Standard EN 50317 [8], which prescribes the use of force transducers located close to the contact interface. The difference between the measured force and the actual contact force is attributed to inertial and aerodynamic effects and is compensated using additional measurements. This approach is widely adopted in industry, with various implementations reported in the literature, such as comparisons between fibre Bragg grating sensors and electrical sensors [2]. Nevertheless, the variability observed in these measurements highlights the intrinsic difficulty of indirect contact force estimation.

Kalman-filter-based techniques [14] are widely used for indirect force estimation in structural dynamics, enabling the reconstruction of unknown excitation forces from noisy displacement, velocity, or acceleration measurements. A commonly adopted strategy is state augmentation, also referred to as the Augmented Kalman Filter (AKF) [12], in which the unknown force is modelled as an additional state driven by a stochastic process. While broadly applicable, the accuracy of this approach strongly depends on the assumed force dynamics, which may lead to over-smoothing or loss of identifiability if improperly modelled. An alternative class of methods consists of unbiased minimum-variance (UMV) estimators [11], which allow simultaneous estimation of system states and unknown inputs without augmenting the state vector [7]. These methods are computationally efficient but require specific conditions on the system matrices. A comprehensive overview of Kalman-filter-based approaches for unknown-input systems is provided by Pan et al. [13], including UMV estimators, projection-based two-stage filters, and extensions to non-linear systems using EKF or UKF formulations.

Kalman-filter-based approaches have also been applied to pantograph systems. In [6], an AKF is used to estimate the contact force from acceleration and displacement measurements using a linear pantograph model with a simplified catenary representation. Camera-based displacement measurements combined with Kalman filtering are considered in [4], where recursive least squares are employed to improve estimation accuracy [10].

Data-driven methods have recently gained attention in this context. Neural networks and recurrent architectures such as LSTM models have been proposed as surrogate models for pantograph–catenary simulations [5, 15–17]. Applications directly related to contact force estimation include ANN-based prediction of contact force statistics from acceleration measurements [9] and hybrid CNN–GRU models trained on simulated data for inverse force estimation [1]. However, experimental validation of such approaches remains limited.

1.4 Research highlights

This paper proposes a fully non-intrusive methodology for estimating the pantograph contact force using acceleration, displacement, and pressure measurements. The pressure signal of the uplift mechanism is exploited to reconstruct the very low-frequency components of the force (below 0.5 Hz), while the remaining frequency content is estimated through inverse dynamic analysis based on motion measurements.

Three Kalman-filter-based formulations are investigated and compared: (1) a standard Augmented Kalman Filter, (2) an Augmented Kalman Filter with coloured noise modelling, and (3) an Augmented Kalman Filter with mixed equations. Since the performance of each approach depends on multiple modelling and tuning parameters, all configurations are optimised to ensure a fair comparison.

The analysis is carried out for two sensing configurations: combined acceleration and displacement measurements, and acceleration-only measurements, allowing the influence of displacement information on estimation accuracy to be assessed. The proposed methodology is experimentally validated using data from a laboratory test bench equipped with a real pantograph, where the estimated contact force is compared with a directly measured reference force.

2 Methodology

The objective of this work is to estimate the contact force acting on a pantograph using a fully non-intrusive approach, i.e., without any structural modification of the pantograph, thereby simplifying implementation with respect to conventional measurement techniques. The proposed methodology is implemented and validated in a laboratory environment using the experimental test bench shown in Fig. 1. The test rig enables: (1) the application of a prescribed vertical displacement to the pantograph through a linear actuator and (2) the direct measurement of the force exerted by the actuator on the pantograph, which is used as reference.

The sensing setup mounted on the pantograph includes: (3) accelerometers installed on the panhead, (4) a displacement sensor measuring the panhead vertical position, and (5) a pressure sensor installed in the uplift mechanism. Unless otherwise stated, all measured signals are low-pass filtered at 20 Hz.

Since constant and very low-frequency forces have a negligible effect on acceleration and displacement responses, contact force estimation is performed by separating the force into low- and high-frequency components, using a cut-off frequency of 0.5 Hz, as illustrated in Fig. 1. The low-frequency component of the contact force, denoted as $f^{\mathrm{Lo}}(t)$, is obtained from the pressure signal of the uplift mechanism. The measured pressure signal $p(t)$ is first low-pass filtered at 0.5 Hz and subsequently mapped to force through a calibrated linear relationship:

$$f^{\mathrm{Lo}}(t) = c_0 + c_1\, p(t),$$

where the coefficients c_0 and c_1 are identified experimentally.

The high-frequency component of the contact force, $f^{\mathrm{Hi}}(t)$, is estimated using Kalman-filter-based inverse dynamic approaches described in Section 2.1. These methods rely on acceleration $a(t)$ and displacement $z(t)$ measurements acquired at the force application point.

The total estimated contact force is finally reconstructed as:

$$f(t) = f^{\mathrm{Lo}}(t) + f^{\mathrm{Hi}}(t),$$

and compared against the reference force $f^*(t)$ measured directly by the test bench.

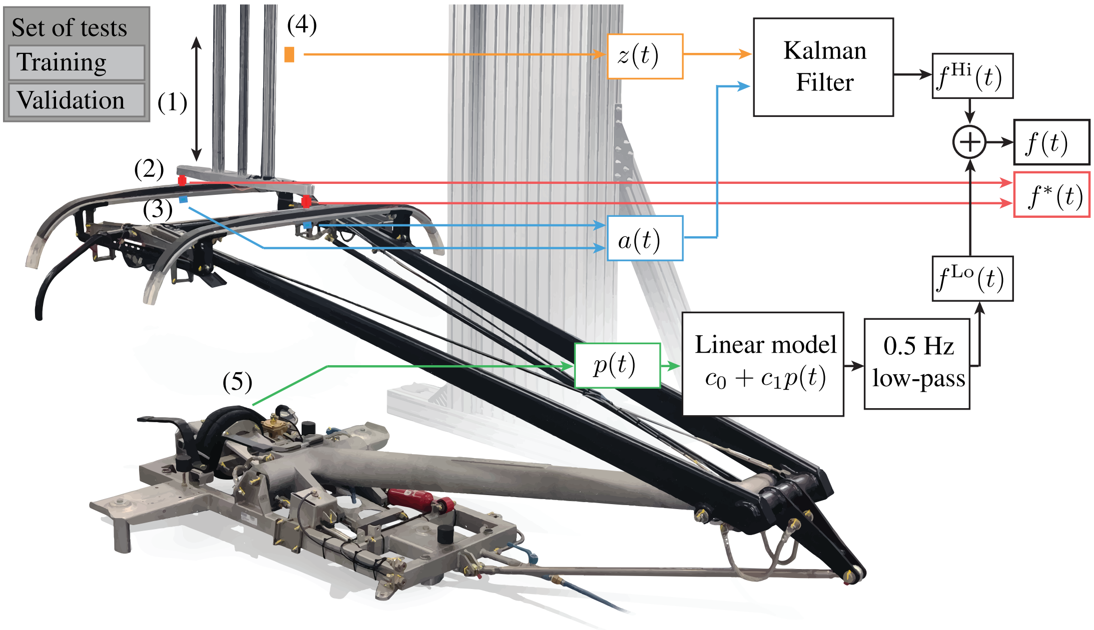

Figure 1: Test bench and indirect measurement set up used in this work.

2.1 Kalman Filter approaches

As summarised in Fig. 1, the Kalman Filter (KF) block is responsible for estimating the high-frequency component of the contact force in the 0.5–20 Hz range. The filter is driven by acceleration and displacement measurements at the pantograph contact point. Although the formulation initially assumes that both measurements are available, an acceleration-only configuration is also investigated.

Three Kalman-filter-based formulations are considered: (1) Augmented Kalman Filter (AKF), (2) Augmented Kalman Filter with coloured noise modelling, and (3) Augmented Kalman Filter with mixed kinematic–dynamic equations.

Kalman filtering is a well-established technique for system state estimation [14], and its augmented formulation enables the simultaneous estimation of unknown external inputs [12]. This makes the AKF particularly suitable for the inverse force estimation problem addressed in this work. As a model-based approach, the method

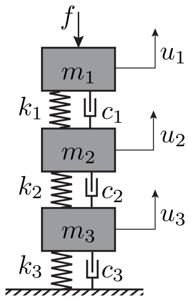

Figure 2: Pantograph linear model.

requires a mechanical model of the pantograph. A commonly adopted three-degree-of-freedom lumped-mass pantograph model [3] is used, consisting of masses, springs, and dampers, as illustrated in Fig. 2.

In contrast to approaches that explicitly model the catenary [6], only the pantograph dynamics are included here, since the relationship between the excitation force and the measured variables can be fully described by the pantograph model. The linear dynamics of the pantograph are governed by:

$$\mathbf{M}\ddot{\mathbf{u}} + \mathbf{C}\dot{\mathbf{u}} + \mathbf{K}\mathbf{u} = \mathbf{S}f, \tag{1}$$

where $\mathbf{M}$, $\mathbf{C}$, and $\mathbf{K}$ denote the mass, damping, and stiffness matrices, respectively, $\mathbf{u}$ is the displacement vector, f is the unknown external force, and $\mathbf{S}$ is the force selection matrix.

Assuming a zero-order hold discretisation, the system can be expressed in discrete-time state-space form as:

$$\mathbf{x}_{k+1} = \mathbf{F}\mathbf{x}_k + \mathbf{G}f_k + \mathbf{w}_k, \tag{2}$$

with the state vector defined as:

$$\mathbf{x}_k = \begin{bmatrix} \dot{\mathbf{u}}_k \\ \mathbf{u}_k \end{bmatrix}, \tag{3}$$

where $\mathbf{w}_k$ represents zero-mean Gaussian process noise with covariance matrix $\mathbf{Q}$. The measurement equation is written as:

$$\mathbf{y}_k = \mathbf{H}\mathbf{x}_k + \mathbf{J}f_k + \mathbf{v}_k, \tag{4}$$

where $\mathbf{v}_k$ is zero-mean Gaussian measurement noise with covariance $\mathbf{R}$.

The state extension can be done by including the external force as an additional state variable. In order to estimate the unknown force f_k, it is modeled as a gaussian process:

$$f_{k+1} = f_k + \eta_k \tag{5}$$

where η_k is a zero-mean Gaussian noise with variance Q_{f} that should be an estimation of the variance of the force increment $\Delta f = f_{k+1} - f_k$.

The augmented state vector is then defined as:

$$\mathbf{x}_k^{\mathrm{a}} = \begin{bmatrix} \dot{\mathbf{u}}_k \\ \mathbf{u}_k \\ f_k \end{bmatrix} \tag{6}$$

Using this augmented state vector, the discrete-time state-space model in Eq. (2) can be rewritten as:

$$\mathbf{x}_{k+1}^{\mathrm{a}} = \underbrace{\begin{bmatrix} \mathbf{F} & \mathbf{G} \\ \mathbf{0} & \mathbf{I} \end{bmatrix}}_{\mathbf{F}_{\mathrm{a}}} \mathbf{x}_k^{\mathrm{a}} + \begin{bmatrix} \mathbf{w}_k \\ \eta_k \end{bmatrix} \tag{7}$$

Similarly, the measurement equation becomes:

$$\mathbf{y}_k = \underbrace{\begin{bmatrix} \mathbf{H} & \mathbf{J} \end{bmatrix}}_{\mathbf{H}_{\mathrm{a}}} \mathbf{x}_k^{\mathrm{a}} + \mathbf{v}_k \tag{8}$$

This augmented formulation allows the simultaneous estimation of the system states and the unknown external force by means of a standard Kalman filter applied to the augmented system.

From this point three different approaches (A1, A2 and A3) can be followed to estimate the contact force.

2.1.1 A1: AKF with acceleration in the measurement

The measurement vector of Eq. (8) consists of the displacement and acceleration at the pantograph contact point, corresponding to u_1 and $\ddot{u}_1$ in the lumped-mass model:

$$\mathbf{y}_k = \begin{bmatrix} \ddot{u}_{1,k} & u_{1,k} \end{bmatrix}^\top \tag{9}$$

While the displacement component can be directly expressed as a linear function of the state vector, the acceleration component must be reformulated using the system dynamics in Eq. (1). To this end, the measurement vector is written as a linear combination of accelerations, velocities, and displacements:

$$\mathbf{y}_k = \mathbf{S}_{\mathrm{a}} \ddot{\mathbf{u}}_k + \mathbf{S}_{\mathrm{v}} \dot{\mathbf{u}}_k + \mathbf{S}_{\mathrm{d}} \mathbf{u}_k. \tag{10}$$

By substituting the acceleration term using Eq. (1), the measurement matrices in Eq. (8) are obtained as:

$$\mathbf{H} = \begin{bmatrix} \mathbf{S}_{\mathrm{v}} - \mathbf{S}_{\mathrm{a}} \mathbf{M}^{-1} \mathbf{C} & \mathbf{S}_{\mathrm{d}} - \mathbf{S}_{\mathrm{a}} \mathbf{M}^{-1} \mathbf{K} \end{bmatrix}, \qquad \mathbf{J} = \mathbf{S}_{\mathrm{a}} \mathbf{M}^{-1} \mathbf{S}. \tag{11}$$

The augmented state-space system defined by Eqs. (7) and (8) can then be estimated using a standard Kalman Filter, with the contact force obtained directly from the augmented state vector.

2.1.2 A2: AKF with coloured noise

In the previous formulation, the unknown contact force is modelled as a random walk driven by white noise, as defined in Eq. (5). However, this assumption may be restrictive when the force exhibits limited bandwidth. To account for this behaviour, the force increment noise is modelled as coloured noise generated by a first-order filter:

$$\eta_{k+1} = A_\mathrm{f}\,\eta_k + \xi_k, \tag{12}$$

where ξ_k is zero-mean Gaussian white noise with covariance Q_ξ.

The coefficient A_f corresponds to a discrete-time low-pass filter and is defined as:

$$A_\mathrm{f} = \exp(-\omega_\mathrm{c}\Delta t), \tag{13}$$

where ω_c denotes the assumed cut-off frequency of the contact force dynamics.

To incorporate this model, the system state vector is further augmented by the coloured noise state, resulting in:

$$\mathbf{x}^\mathrm{a}_{k+1} = \begin{bmatrix} \mathbf{F} & \mathbf{G} & \mathbf{0} \\ \mathbf{0} & 1 & 1 \\ \mathbf{0} & 0 & A_\mathrm{f} \end{bmatrix} \mathbf{x}^\mathrm{a}_k + \begin{bmatrix} \mathbf{w}_k \\ \mathbf{0} \\ \xi_k \end{bmatrix}, \tag{14}$$

with the augmented state vector defined as:

$$\mathbf{x}^\mathrm{a}_k = \begin{bmatrix} \mathbf{x}_k & f_k & \eta_k \end{bmatrix}^\top.$$

The corresponding measurement equation becomes:

$$\mathbf{y}_k = \begin{bmatrix} \mathbf{H} & \mathbf{J} & \mathbf{0} \end{bmatrix} \mathbf{x}^\mathrm{a}_k + \mathbf{v}_k, \tag{15}$$

where the measurement matrices $\mathbf{H}$ and $\mathbf{J}$ are identical to those defined in Eq. (11). A standard Kalman Filter applied to this augmented system yields simultaneous estimates of the system states and the contact force.

2.1.3 A3: AKF with mixed kinematic–dynamic formulation

In this approach, acceleration measurements are treated as known inputs to the estimation problem rather than as outputs of the dynamic model.

The degrees of freedom (d.o.f.) are divided into two groups. Group a includes the d.o.f. for which acceleration measurements are available, while group b contains the remaining d.o.f. The displacement vector is partitioned as $\mathbf{u} = [\mathbf{u}_a \mathbf{u}_b]^\top$. The equations of motion in Eq. (1) are accordingly partitioned as:

$$\begin{bmatrix} \mathbf{M}_{aa} & \mathbf{M}_{ab} \\ \mathbf{M}_{ba} & \mathbf{M}_{bb} \end{bmatrix} \begin{bmatrix} \ddot{\mathbf{u}}_a \\ \ddot{\mathbf{u}}_b \end{bmatrix} + \begin{bmatrix} \mathbf{C}_{aa} & \mathbf{C}_{ab} \\ \mathbf{C}_{ba} & \mathbf{C}_{bb} \end{bmatrix} \begin{bmatrix} \dot{\mathbf{u}}_a \\ \dot{\mathbf{u}}_b \end{bmatrix} + \begin{bmatrix} \mathbf{K}_{aa} & \mathbf{K}_{ab} \\ \mathbf{K}_{ba} & \mathbf{K}_{bb} \end{bmatrix} \begin{bmatrix} \mathbf{u}_a \\ \mathbf{u}_b \end{bmatrix} = \begin{bmatrix} \mathbf{f}_a \\ \mathbf{f}_b \end{bmatrix}. \tag{16}$$

For the d.o.f. in group a, the dynamic equations are replaced by kinematic state-space relations:

$$\begin{bmatrix} \ddot{\mathbf{u}}_a \\ \dot{\mathbf{u}}_a \end{bmatrix} = \begin{bmatrix} \mathbf{0} & \mathbf{0} \\ \mathbf{I} & \mathbf{0} \end{bmatrix} \begin{bmatrix} \dot{\mathbf{u}}_a \\ \mathbf{u}_a \end{bmatrix} + \begin{bmatrix} \mathbf{I} \\ \mathbf{0} \end{bmatrix} \mathbf{a}_a, \tag{17}$$

where $\mathbf{a}_a$ denotes the measured acceleration.

By combining the kinematic equations for group a and the dynamic equations for group b, the continuous-time state-space system is obtained and it can be written in discrete time scheme in the shape of Eq. (2).

In this work, acceleration and displacement measurements are available only for the first degree of freedom, which therefore belongs to group a. External forces acting on the remaining degrees of freedom are assumed to be zero.

The system output is defined as the displacement of group a: $\mathbf{y} = \mathbf{u}_a + \mathbf{v}$, where $\mathbf{v}$ denotes zero-mean Gaussian measurement noise with covariance $\mathbf{R}$.

The Kalman Filter uses the measured acceleration as an input and the measured displacement for the correction step. After estimating the system states, the contact force acting on group a is recovered in a post-processing step using the dynamic equilibrium:

$$\mathbf{f}_a = \mathbf{M}_{aa}\ddot{\mathbf{u}}_a + \mathbf{C}_{aa}\dot{\mathbf{u}}_a + \mathbf{K}_{aa}\mathbf{u}_a + \mathbf{M}_{ab}\ddot{\mathbf{u}}_b + \mathbf{C}_{ab}\dot{\mathbf{u}}_b + \mathbf{K}_{ab}\mathbf{u}_b, \tag{18}$$

where the acceleration of group b is obtained from:

$$\ddot{\mathbf{u}}_b = \mathbf{M}_{bb}^{-1}\left(\mathbf{f}_b - \mathbf{M}_{ba}\mathbf{a}_a - \mathbf{C}_{bb}\dot{\mathbf{u}}_b - \mathbf{K}_{bb}\mathbf{u}_b - \mathbf{C}_{ba}\dot{\mathbf{u}}_a - \mathbf{K}_{ba}\mathbf{u}_a\right). \tag{19}$$

3 Optimisation

The performance of the Kalman Filter approaches described in Section 2.1 depends on a set of user-defined parameters. In this work, these parameters are determined through an optimisation procedure to ensure that each approach is evaluated under its best achievable performance, enabling a fair comparison. While most parameters are optimised, some are fixed based on physical considerations or to limit computational cost.

Certain parameters can be estimated directly from measured signals. In particular, the process noise associated with the contact force represents the variance of the force increments. In the pantograph-catenary interaction, the acceleration of the upper mass m_1 largely dominates the contact force dynamics. Assuming $f \approx m_1 a$, the process noise for the contact force can be approximated as:

$$Q_\mathrm{f} = \mathrm{Var}(\eta_k), \quad \text{with } \eta_k = f_{k+1} - f_k. \tag{20}$$

For the coloured-noise Kalman Filter (A2), the noise variance Q_η is similarly estimated from the filtered increments:

$$Q_\eta = \mathrm{Var}(\xi_k), \quad \text{with } \xi_k = \eta_{k+1} - A_\mathrm{f}\eta_k = f_{k+2} - f_{k+1} - A_\mathrm{f}(f_{k+1} - f_k). \tag{21}$$

To reduce the number of optimisation variables, the process noise and measurement covariance matrices $\mathbf{Q}$ and $\mathbf{R}$ are assumed diagonal and identical across all degrees of freedom:

$$\mathbf{Q} = \begin{bmatrix} Q_{\mathrm{v}}\mathbf{I}_3 & \mathbf{0} \\ \mathbf{0} & Q_{\mathrm{u}}\mathbf{I}_3 \end{bmatrix}, \quad \mathbf{R} = \begin{bmatrix} R_{\mathrm{a}} & 0 \\ 0 & R_{\mathrm{z}} \end{bmatrix}, \tag{22}$$

where Q_{v}, Q_{u} are the process noise variances for velocity and displacement, and R_{a}, R_{z} are the measurement noise variances for acceleration and displacement.

The parameters optimised in this study include the pantograph model coefficients, the cut-off frequency of the coloured-noise filter (for A2 only), and the diagonal noise covariances: k_1, k_2, k_3,c_1, c_2, c_3,m_1, m_2, m_3, ω_{c}, Q_{v}, Q_{z}, R_{a} and R_{a}.

The optimisation procedure is illustrated in Fig. 3. Each approach is trained independently on the training set. The predicted contact force (high-frequency component above 0.5 Hz) is compared with the measured force, and the error is computed. The optimisation algorithm iteratively adjusts the parameters to minimise this error.

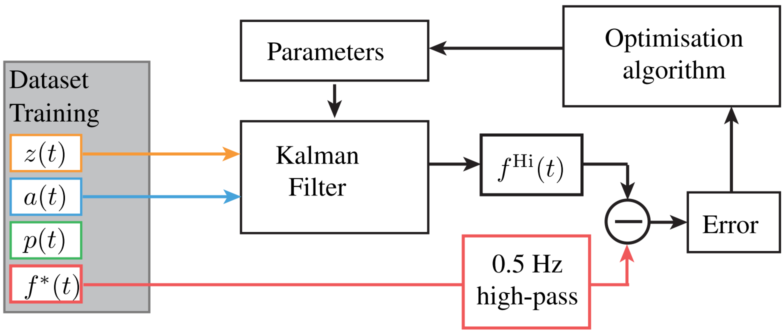

Figure 3: Parameter optimisation strategy.

A Genetic Algorithm (GA) is employed for parameter optimisation. GA is a population-based global optimisation method suitable for high-dimensional problems with complex objective functions. The algorithm starts from an initial population centred around nominal parameter values. Over multiple generations, selection and variation operators evolve the population toward lower prediction errors. Parameter bounds are enforced, and parallel evaluation accelerates computation. The optimisation is run for sufficient generations to converge toward a global or near-global minimum of the contact force prediction error.

4 Results

The parameter optimisation described in Section 3 is performed using the dataset presented below. The performance of the different Kalman Filter approaches is then compared. Finally, to validate the methodology for low-frequency contact force prediction, tests with varying pantograph uplift pressure are performed.

Three types of displacement signals are imposed on the pantograph to generate the dataset. **Chirp signal**: frequency increases linearly with time while amplitude decreases linearly, different amplitudes are use for the training dataset. **Pseudo signal**: superposition of harmonic functions with random phases, different amplitudes are use for the training dataset. **Catenary signal**: displacement of the contact wire from simulated pantograph-catenary interaction at different velocities, 225 and 300 km/h for the training dataset and 250 and 275 km/h for the validation dataset.

The normalized root mean square error (NRMSE) is used to evaluate the performance of the different Kalman Filter approaches in predicting the contact force.

Figure 4 compares the NRMSE for approaches A1, A2, and A3 across both Problem 1 (acceleration + displacement measurements) and Problem 2 (acceleration only). Results are reported separately for training and validation datasets. Approach A3 (AKF with mixed formulation) achieves the lowest error. Importantly, there is no significant increase in error when using only acceleration measurements (Problem 2), indicating that the method can be effectively applied without displacement sensors.

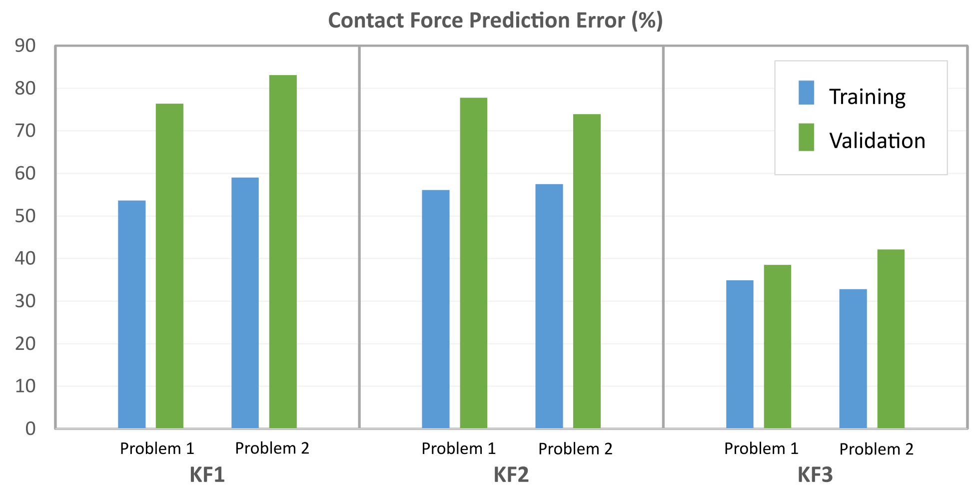

Figure 4: Comparison of different Kalman Filter strategies (A1, A2, A3) in terms of NRMSE. Results are shown for training and validation datasets for both Problem 1 and Problem 2.

In order to illustrate the temporal fitting between prediction and real force, Fig. 5 shows representative time histories of the predicted and measured contact force using approach A3 for the validation dataset in Problem 2, respectively.

The contact force below 0.5 Hz is estimated from the pressure measurement of the pantograph uplift mechanism (Fig. 1). To validate this, a test is conducted with varying pressure in the mechanism. Figure 6 shows the predicted contact force obtained by combining the low-frequency component from the pressure measurement with the high-frequency prediction from approach A3 (Problem 1). The moving average of the contact force is accurately captured, demonstrating the efficacy of this approach for low-frequency force reconstruction.

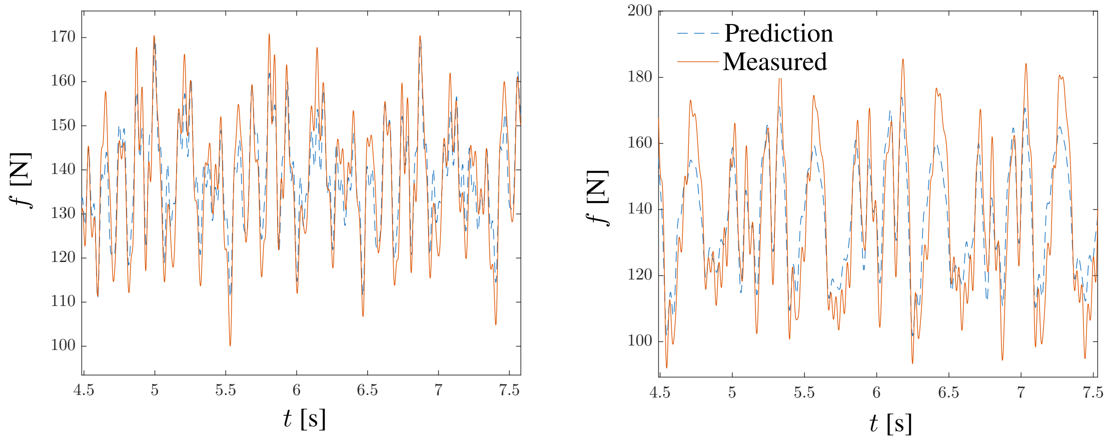

Figure 5: Approach A3 for validation tests of Problem 2: catenary signals at 250 km/h and 275 km/h.

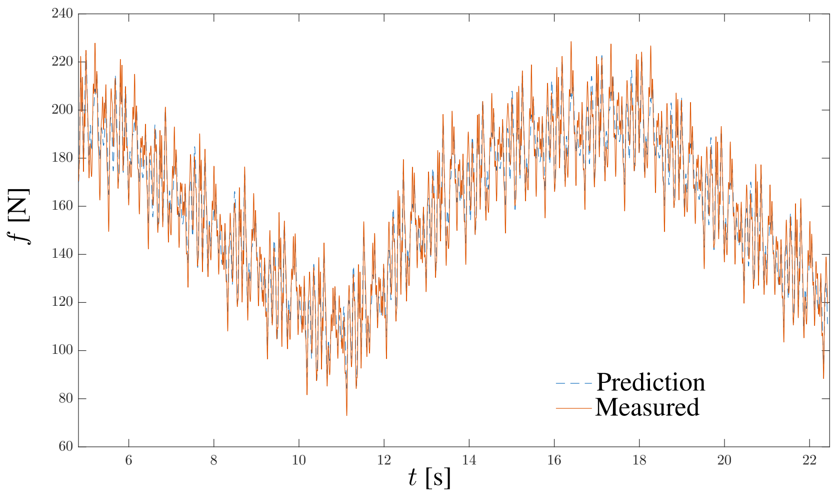

Figure 6: Approach A3 for validation test of Problem 1: catenary signal at 250 km/h with pressure variations.

5 Concluding remarks

This work addressed the problem of estimating the contact force acting on a railway pantograph by means of a fully non-intrusive approach, avoiding any structural modification of the system. The proposed methodology combines pressure measurements from the uplift mechanism with displacement and acceleration measurements on the panhead, enabling the reconstruction of the contact force over the frequency range of interest defined by EN 50317 [8].

A two-stage estimation strategy was introduced, in which the very low-frequency component of the contact force is obtained from the pressure signal through a calibrated linear relationship, while the higher-frequency content is reconstructed from acceleration and displacement measurements using inverse dynamic models. This separation was shown to be necessary, as the other measurements alone cannot provide information on the mean force level or on very low-frequency components.

The Kalman Filter is used with three different approaches. The comparison was carried out under identical experimental conditions and with parameter optimisation for each approach, ensuring a fair assessment of their best achievable performance. Furthermore, two measurement configurations were analysed—acceleration combined with displacement, and acceleration-only (allowing the influence of displacement measurements on estimation accuracy to be quantified).

The implementation was performed on a laboratory test bench with a real pantograph and a directly measured contact force for assessing the method. The results demonstrate that the proposed non-intrusive framework is capable of reconstructing the contact force with good accuracy within the target frequency range. The study also highlights the non-necessity of including displacement measurements for contact force estimation.

Acknowledgements

The authors would like to express their gratitude for the financial support received from the State Research Agency of the Spanish Science and Innovation Ministry (PID2023-148854OB-C21).

References

[1] Laha Ale, Yang Song, Zhigang Liu, Huanlai Xing, and Hongbin Liang. Real-time prediction of high-speed rail pantograph-catenary contact force using deep learning framework. *Vehicle System Dynamics*, 0(0):1–23, 2026.

[2] Marco Bocciolone, Giuseppe Bucca, Andrea Collina, and Lorenzo Comolli. Comparison of optical and electrical measurements of the pantograph-catenary contact force. In José Luís Santos, Brian Culshaw, José Miguel López-Higuera, and William N. MacPherson, editors, *Fourth European Workshop on Optical Fibre Sensors*, volume 7653, page 765346. International Society for Optics and Photonics, SPIE, 2010.

[3] Stefano Bruni, Jorge Ambrosio, Alberto Carnicero, Yong Hyeon Cho, Lars Finner, Mitsuru Ikeda, Sam Young Kwon, Jean Pierre Massat, Sebastian Stichel, and Manuel Tur. The results of the pantograph-catenary interaction benchmark. *Vehicle System Dynamics*, 53(3):412–435, 2015.

[4] Hongming Chen, Ning Zhou, and Weihua Zhang. Non-contact contact force estimation for pantograph and catenary system based on kalman filter. In Wei Huang and Mehdi Ahmadian, editors, *Advances in Dynamics of Vehicles on Roads and Tracks III*, pages 41–50, Cham, 2025. Springer Nature Switzerland.

[5] Wenping Chu, Hui Wang, Yang Song, and Zhigang Liu. Fenet: A physics-informed dynamics prediction model of pantograph-catenary systems in electric railway. *IET Intelligent Transport Systems*, 19(1):e70059, 2025.

[6] A. Collina, F. Fossati, M. Papi, and F. Resta. Impact of overhead line irregularity on current collection and diagnostics based on the measurement of pantograph dynamics. *Proceedings of the Institution of Mechanical Engineers, Part F: Journal of Rail and Rapid Transit*, 221(4):547–559, 2007.

[7] M. Darouach, M. Zasadzinski, and M. Boutayeb. Extension of minimum variance estimation for systems with unknown inputs. *Automatica*, 39(5):867–876, 2003.

[8] EN 50317. Railway applications. Current collection systems. Requirements for and validation of measurements of the dynamic interaction between pantograph and overhead contact line. *European Committee for Electrotechnical Standardization*, 2012.

[9] S. Gregori, M. Tur, J. Gil, and F. J. Fuenmayor. Assessment of catenary condition monitoring by means of pantograph head acceleration and artificial neural networks. *MECHANICAL SYSTEMS AND SIGNAL PROCESSING*, 202, NOV 1 2023.

[10] Chih-Chergn Ho and Chih-Kao Ma. Active vibration control of structural systems by a combination of the linear quadratic gaussian and input estimation approaches. *Journal of Sound and Vibration*, 301(3):429–449, 2007.

[11] Peter K. Kitanidis. Unbiased minimum-variance linear state estimation. *Automatica*, 23(6):775–778, 1987.

[12] E. Lourens, E. Reynders, G. De Roeck, G. Degrande, and G. Lombaert. An augmented kalman filter for force identification in structural dynamics. *Mechanical Systems and Signal Processing*, 27:446–460, 2012.

[13] Shuwen Pan, Pengying Du, Yanjun Li, Zuo Chen, and Hong Wang. The study on an general kalman filter with unknown inputs. In *Proceeding of the 11th World Congress on Intelligent Control and Automation*, pages 3562–3567, 2014.

[14] Dan Simon. *Optimal State Estimation: Kalman, H Infinity, and Nonlinear Approaches*. Wiley-Interscience, 2006.

[15] Yang Song, Hongrui Wang, Gunnstein Frøseth, Petter Nåvik, Zhigang Liu, and Anders Rønnquist. Surrogate modelling of railway pantograph-catenary interaction using deep long-short-term-memory neural networks. *Mechanism and Machine Theory*, 187:105386, 2023.

[16] Mengzhen Wu, Xianghong Xu, Haochen Zhang, Rui Zhou, and Jianshan Wang. Pantograph–catenary interaction prediction model based on scsa-rbf network. *Applied Sciences*, 14(1), 2024.

[17] Rui Zhou and Xianghong Xu. Contact force surrogate model and its application in pantograph–catenary parameter optimization. *Applied Sciences*, 14(1), 2024.